Tactile Perception using Micro Force/Moment Sensor Embedded in Soft Fingertip

Ikuo Fujii, Takahiro Inoue, Dzung Viet Dao, Susumu Sugiyama, and Shinichi Hirai
Department of Robotics, Ritsumeikan Univ.,
1-1-1 Noji-Higashi, Kusatsu, Shiga 525-8577, Japan
rr010015@se.ritsumei.ac.jp

***Abstract*— In this paper, we show a novel tactile sensor fabricated by embedding a Micro-Force/Moment Sensor inside a hemispherical soft fingertip, which is applicable to the object manipulation using robotic hands. This sensor is produced by MEMS technology, designed to detect one force component (*Fz*) and two moment components (*Mx,My*). The structure is composed of a central square-block and four crisscross beams across the block, and its dimension is 9 mm^2 for a single sensing chip. We designed two types piezoresistors on the beams. One is a conventional two-terminal piezoresistor capable to measure a longitudinal strain, and the other is a four-terminal square-shaped piezoresistor capable to measure a transverse strain. We also applied a structural analysis to the chip to evaluate stress distribution on it. Finally, we show that *Fz,Mx*, and *My* measured by the electrical potential difference on each terminal have high accuracy and keep low fluctuation in compression test of the soft fingertip.**

***Index Terms*— Tactile sensor, Grasping, Manipulation, MEMS, Piezoresistor, Force/moment sensor, Soft fingertip.**

I. Introduction

Soft-fingered manipulation has much potential to simplify the explanation of secure grasping mechanism in human and the design of control system of robotic hands with soft fingers.

Inoue *et al.* [1], [2] have proposed a quasi-static manipulation method based on the concept of "*local minimum of elastic potential energy* (LMEE)" on a hemispherical soft fingertip. Their study clarified that the object position and posture grasped by two rotational soft fingers are determined uniquely without any control input because the grasped object consistently comes to rest stably at an LMEE. This invaluable secure grasping comes from the softness of a full rubber and solid fingertip structure, not from a rubber coating structure on a rigid fingertip. In order to make full use of the characteristics of the solid-rubber fingertip, we need to microminiaturize an individual sensor used for being embedded into the soft fingertip.

This study shows a novel micro-force/moment sensor produced by using MEMS technology, which is able to detect six forces and moments [3]. Furthermore, we present a tactile sensor-embedded soft fingertip (TES) using a type of three-axes force/moment sensing chip that is improved for the use of application of tactile perception. The conventional sensing chip is composed of cross-shaped four beams that is designed by linear elastic theory and FEM analysis [3]. Additionally, eighteen piezoresistors are placed on the beams in an uniform rule, which are able to measure the longitudinal and shear stresses externally applied. Finally, we conduct a static compression test for the TES, and demonstrate that the sensor can detect the subtle force and moment and has an outstanding sensitivity to recognize the forces.

II. Design of Micro Force/Moment Sensor

We describe the design of a six-degree of freedom force/moment micro sensing chip using the piezoresistance effect in silicon. The sensing chip is designed to be able to simultaneously detect three components of force and three components of moment in three orthogonal directions.

The sensing chip is a single crystalline crossbeam with piezoresistors diffused on the surface of the four suspended-beams. Forces and moments applied to the sensing chip, shown in Fig.1 and Fig.2, deform the four beams and change the resistance of the piezoresistors, which leads to a change in output of corresponding measurement circuits. The beam's dimension, piezoresistance coefficients and the positions of piezoresistors on the sensing chip are the main factors determining the sensitivity of the sensor.

In this section, we describe the structural analysis of the sensing chip, which is based on classical elasticity theory

A. The case when F_z is applied to the sensing chip

The sensing chip is composed of four beams and a central block as shown in Fig.1. Let us consider a force F_z is applied to the central point O. The stress states in the four beams are similar because of symmetry of the model. The problem can be simplified to the case of a beam that is fixed at one end, and free but guided to z axis at the other with load $F_z/4$, as shown in Fig.3-(a). The cross-sectional plane at the free end is always vertical, therefore, there is no angular deformation. The general equation for longitudinal stress at any point can be written by

$$\sigma_L(x) = \frac{F_z}{4Z_Y}\left(\frac{L}{2} - x\right), \tag{1}$$

$$Z_Y = \frac{I_Y}{t/2} = \frac{wt^2}{6}, \tag{2}$$

where I_Y, Z_Y are the moment of inertia of the cross-sectional area with respect to the Y axis and corresponding section modulus, respectively. The longitudinal stress σ_L

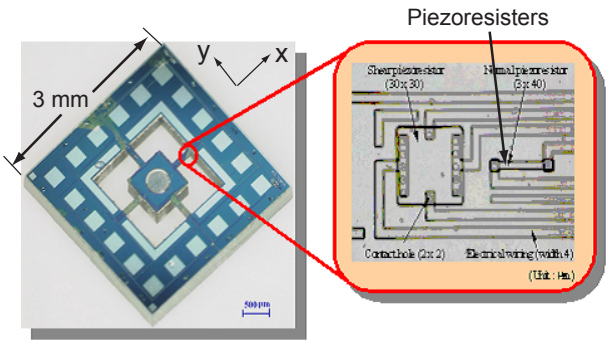

Fig. 1. Sensing chip fabricated by using MEMS technology

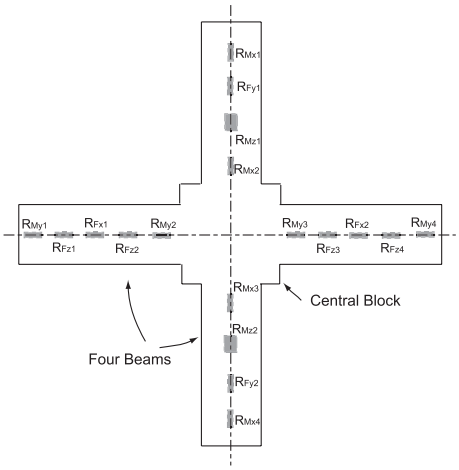

Fig. 2. Design of 18 piezoresistors

on the beam's surface reaches maximum at both ends of the beam and zero at the center, as shown in Fig.3-(b). The deflection at any point can be represented as

$$\delta z = \frac{F_z \cdot x^2}{48 E_X I_Y}(3L - 2x), \tag{3}$$

$$\delta z_{max} = \frac{F_z \cdot L^3}{48 E_X I_Y}, \tag{4}$$

where E_X is the Young's modulus of single crystal silicon in X direction.

B. The case when $M_x(M_y)$ is applied to the sensing chip

When a moment M_y around the Y axis is applied to the central block of the sensing chip, the beams A and B are bent, while the beams C and D are purely twisted. By symmetry, we need only to consider the stress states in the beams A and D. The stresses in the beams B and C are equal in magnitude but opposite in sign with those of the beams A and D, respectively. Fig.4 shows the reaction forces and moments acting on each member (beam A, beam D, and central block).

The displacement in Z direction, δz, and slope angle, θ, of the free end of the beam A due to moment M_{RY} and

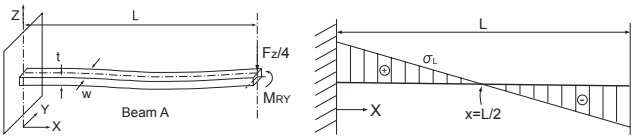

(a) deflection (b) stress distribution

Fig. 3. Analytical model of a beam in F_z

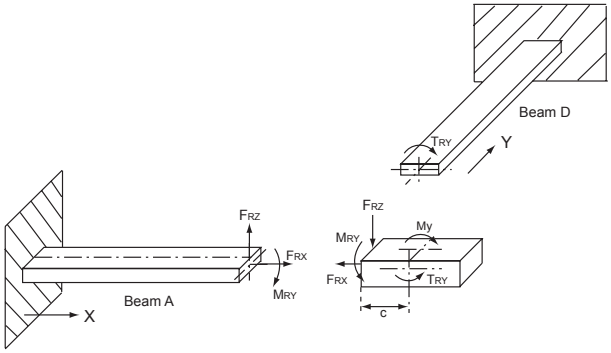

Fig. 4. Analytical model of a beam in $M_x(M_y)$

force F_{RZ} can be written by

$$\delta z = \frac{F_{RZ} \cdot L^3}{3E_X I_Y} - \frac{M_{RY} \cdot L^2}{2E_x I_Y}, \tag{5}$$

$$\theta = \frac{M_{RY} \cdot L}{E_X I_Y} - \frac{F_{RZ} \cdot L^2}{2E_x I_Y}, \tag{6}$$

The central block is also rotated around the original point O by the angle θ, therefore, the displacements of the free end can be expressed as

$$\delta z \simeq c\theta, \tag{7}$$

$$\delta x \simeq c\theta^2. \tag{8}$$

Substituting Eqs. (7) and (8) into Eqs. (5) and (6), the force F_{RZ} and moment M_{RY} can be written by

$$F_{RZ} = \frac{12 E_X I_Y}{L^3}\left(c + \frac{L}{2}\right)\theta, \tag{9}$$

$$M_{RY} = \frac{12 E_X I_Y}{L^2}\left(\frac{c}{2} + \frac{L}{3}\right)\theta, \tag{10}$$

$$F_{RX} = \frac{wtE_X}{L} c\theta^2. \tag{11}$$

Note that the free end of the beam D is also rotated by angle θ (equal to the rotation angle of the central block around the$Y$ axis). The stress state in this beam is equivalent to the case in which a square-cross-sectional surface with one end is fixed , and be purely twisted at the free end by a torque moment T_{RY}. The value of torque moment T_{RY} applied at the free end of the beam D can be represented as [4]

$$T_{RY} = \frac{KG}{L}\theta, \tag{12}$$

where G is shear modulus, and K is the geometric factor of the beam, which is determined by the experimental

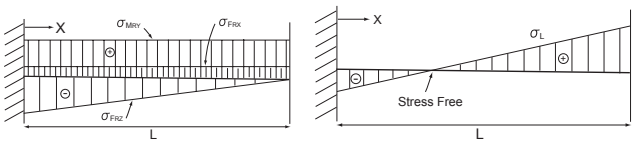

(a) individual stress (b) total stress σ_L

Fig. 5. Stress distribution when the $M_x(M_y)$ is applied to the central block

formula:

$$K = \frac{wt^3}{16}\left\{\frac{16}{3} - 3.36\frac{t}{w}\left(1 - \frac{t^4}{12w^4}\right)\right\}. \quad (13)$$

Now, the moment equilibrium of the central block can be expressed as

$$M_y = 2(M_{RY} + T_{RY} + F_{RZ}\cdot c). \quad (14)$$

Substituting Eqs. (9), (10), and (12) into Eq. (14), the deformed angle θ can be calculated as

$$\theta = \frac{1}{2}\cdot\frac{M_y}{\frac{12E_XI_Yc}{L^3}\left(c+\frac{L}{2}\right) + \frac{12E_XI_Y}{L^2}\left(\frac{c}{2}+\frac{L}{3}\right) + \frac{KG}{L}}. \quad (15)$$

Finally, the equation of the longitudinal stresses on the surface of the beam A induced by moment M_{RY}, forces F_{RZ}, and F_{RX} can be respectively written by

$$\sigma_{M_{RY}}(x) = \frac{M_{RY}t}{2I_Y} = \frac{6E_Xt\theta}{L^2}\left(\frac{c}{2}+\frac{L}{3}\right), \quad (16)$$

$$\sigma_{F_{RZ}}(x) = -\frac{F_{RZ}(L-x)t}{2I_Y} = -\frac{6E_Xt\theta}{L^3}(c+\frac{L}{2})(L-x), \quad (17)$$

$$\sigma_{F_{RX}}(x) = \frac{F_{RX}}{wt} = \frac{E_Xc\theta^2}{L} \geq 0. \quad (18)$$

By applying the superposition method, the total longitudinal stress on the surface of the beam A is then represented as follows:

$$\sigma_L(x) = \sigma_{M_{RY}}(x) + \sigma_{F_{RZ}}(x) + \sigma_{F_{RX}}(x). \quad (19)$$

Fig. 5-(a) shows the distributions of the longitudinal stresses $\sigma_{M_{RY}}, \sigma_{F_{RZ}}, \sigma_{F_{RX}}$, and Fig. 5-(b) shows the total longitudinal stress σ_L represented in Eq. (19).

The stresses at the fixed end $(x=0)$ and free end $(x=L)$ can be expressed as

$$\sigma_L(0) = -\frac{6E_Xt\theta}{L^2}\left(\frac{L}{6}+\frac{c}{2}\right) + \frac{E_Xc\theta^2}{L}, \quad (20)$$

$$\sigma_L(L) = \frac{6E_Xt\theta}{L^2}\left(\frac{L}{3}+\frac{c}{2}\right) + \frac{E_Xc\theta^2}{L}. \quad (21)$$

The stress-free point can be found by solving Eq. (19), $\sigma_L(x) = 0$.

$$x_{\sigma=0} = \frac{L}{2c+L}\left(\frac{L+3c}{3} + \frac{Lc\theta}{3t}\right). \quad (22)$$

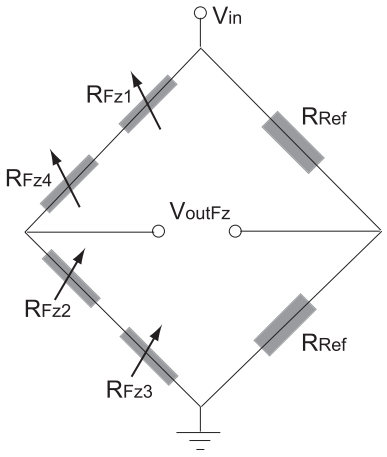

Fig. 6. Wheatstone bridge to measure the force F_z

III. Detection Principle

As shown in Fig.2, eighteen piezoresistors are designed on the surface of all beams, which are distinguished into two types of piezoresistors; one detects longitudinal stresses and the other does shear stresses. Furthermore, input/output terminals for measuring the forces and moments $(F_x, F_y, F_z, M_x, M_y, M_z)$ are arranged on the outer frame of the sensing chip, as shown in Fig.1. As an example, we explain a detection principle of F_z that can be independently measured from the other signals.

Fig.6 shows a wheatstone bridge to measure the force F_z. Since two reference resistors R_{Ref} are identical and constant and all the piezoresistors R_{Fzi} are designed to be identical, this is a half bridge and be balanced at stress-free state. When the resistances of piezoresistors $R_{F_{zi}}$ are changed due to stress, the output voltage of F_z-bridge is expressed by

$$V_{outFz} = \frac{r}{(1+r)^2}\left(\frac{\Delta R_{F_{z1}} + \Delta R_{F_{z4}}}{R_{F_{z1}} + R_{F_{z4}}} - \frac{\Delta R_{F_{z2}} + \Delta R_{F_{z3}}}{R_{F_{z2}} + R_{F_{z3}}}\right)V_{in}, \quad (23)$$

where

$$r = \frac{R_{F_{z1}} + R_{F_{z4}}}{R_{F_{z2}} + R_{F_{z3}}} = 1. \quad (24)$$

When a vertical force F_z is applied to the sensing chip, the longitudinal stresses in the four piezoresistors of the F_z-bridge can be written from Eq. (1) as follows:

$$\sigma_{R_{Fz1}} = \sigma_{R_{Fz4}} = -\sigma_{R_{Fz2}} = -\sigma_{R_{Fz3}}, \quad (25)$$

where $\sigma_{R_{Fzi}}$ is the longitudinal stress at piezoresistors $R_{F_{zi}}(i = 1-4)$. Therefore, the following relationship is satisfied.

$$\Delta R_{F_{z1}} = \Delta R_{F_{z4}} = -\Delta R_{F_{z2}} = -\Delta R_{F_{z3}}. \quad (26)$$

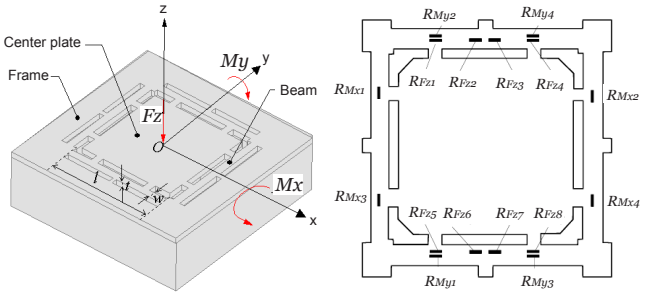

(a) structure (b) layout of piezoresistors

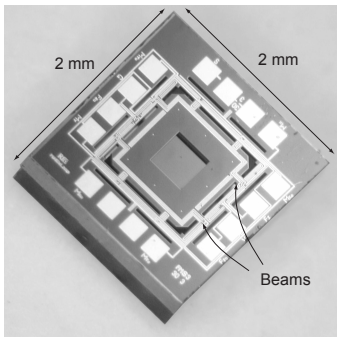

(c) sensing chip

Fig. 7. Improved new micro force/moment sensor.

TABLE I
MAXIMUM FORCE AND MOMENT.

Strength	Force [mN]	Moment [N·μm]
	5000	800
Sensitivity	S_{Fz} [mV/mN]	S_{Mx}, S_{My} [mV/(N·μm)]
	0.2	2.83

Consequently, the F_z-bridge is unbalanced, and the output response appears. For the F_z-bridge, the output voltage represented in Eq. (23) can finally be expressed by

$$V_{outFz} = \frac{1}{2}\frac{\Delta R_{F_{z1}}}{R_{F_{z1}}} V_{in}. \tag{27}$$

IV. IMPROVED MICRO FORCE/MOMENT SENSOR AND ITS PACKAGING

For the application by means of a robotic hand equipped with tactile sensors, we have to redesign a refined sensor having high sensitivity and increase the intensity of the sensor. In the present section, we show an improved micro force/moment sensor that has high sensitivity and strength, as shown in Fig.7 and Table I.

In this sensor the piezoresistors are placed as shown in Fig.7-(b), and the potential difference that is generated by applying force to the sensor can be measured by the corresponding bridge circuit designed within the sensing chip. As shown in Fig.7-(c), a set of power electrode and the electrodes for measuring (Fz, Mx, My) are laid out around the sensing chip.

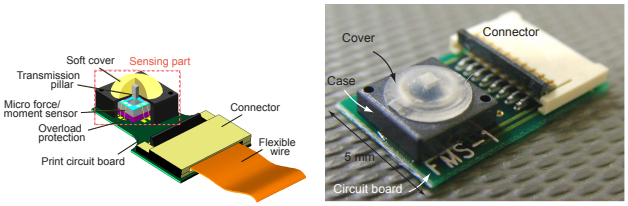

(a) schematic of the sensor (b) tactile sensor

Fig. 8. A novel tactile sensor packaged for sensing slight change of force and moment.

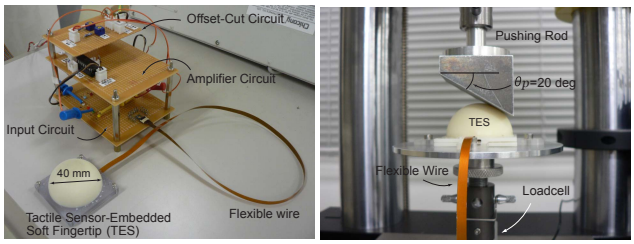

(a) overall view of TES (b) compression test

Fig. 9. Setup of tactile sensor-embedded soft fingertip (TES).

In addition, as shown in Fig.8 we show a tactile sensor packaged for the use of applications, for example: measuring the slight force in contact with some sort of object and the inner force/pressure within soft materials, etc. This tactile sensor is able to detect the external force applied through a soft and thin rubber covered the sensing chip. The detecting mechanism is that the applied force first transmits to a pillar through the soft rubber, as shown in Fig.8-(a). Continuously, the pillar placed on the central stage of the sensing chip shown in Fig.7-(c) yields the combined bending and tortional deflections on each beam.

V. TACTILE SENSOR-EMBEDDED SOFT FINGERTIP (TES)

A. Structure and Setup

This study provides a novel *T*actile sensor-*E*mbedded *S*oft fingertip that is abbreviated as TES, which is necessary for the tactile feedback required for the acquirement of human-like manipulation ability using a robotic soft-fingered hand.

Fig.9-(a) shows a TES system that consists of an input circuit, a amplifier circuit, an offset-cut circuit, and the TES itself. The voltage gain of the amplifier circuit is approximately 3000-fold.

B. Compression Test

We conduct the compression test of a TES as shown in Fig.9-(b), and demonstrate the high performance and excellent dynamic response of the sensor. In this test, a pushing rod that inclines by 20 deg makes contact with the TES, and we increase the applied force until the loadcell placed on the compression machine marks 60 N, as shown in Table II and Fig.10-(a). Furthermore, the rod is in contact

TABLE II

INPUT MANNER OF THE APPLIED FORCE IN COMPRESSION

Timing	Motion manner of pushing rod
Test start	20 mm/min compression
Max force (60 N)	0 mm/min (Test stops)
Up to push "Return"	0 mm/min (Stopping)
After push "Return"	The rod returns rapidly to initial position

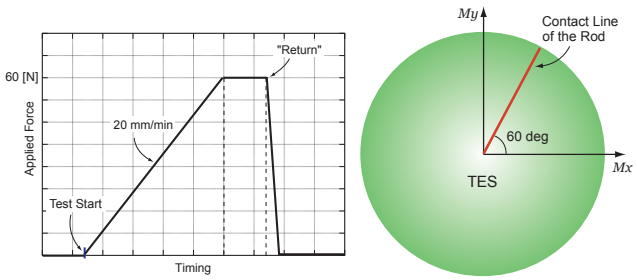

(a) motion of the rod (b) contacting angle

Fig. 10. Motion manner of the pushing rod of the compression machine.

with the soft fingertip keeping 60 deg from the x-axis, as illustrated in Fig.10-(b). The results of (Fz, Mx, My) measured by the TES are plotted in Fig.11 and Fig.12, and Fz in the contact of $\theta_p = 0$ is also depicted in Fig.11-(a) for comparison. Note that the starting point of the compression is not consistent in every figure because it is difficult to synchronize the onset of compression and electrical measurement of the output voltage of TES. In addition, the output voltage in the figures is previously amplified by 3000 times.

As shown in Fig.11 and Fig.12, each output voltage increases with a certain power law against the linearly-applied force. The Fz voltage when $\theta_p = 20$ deg is larger than that in $\theta_p = 0$. This result comes from the fact that the local minimum of elastic potential energy (LMEE) on hemispherical soft fingertip exists [1], [2]. While the speed of response is good enough to follows the rod's return, the the voltage gradually decreases to the initial value when the time is approximately 36 sec and 35 sec in Fig.11-(a) and Fig.11-(b), respectively. This means that the shape variation of soft fingertip cannot follow the rapid rod's return.

As shown in Fig.12, the voltage of Mx is larger than that of My. It is because that the contacting rod is placed at the position inclined by 60 deg from the x-axis, as illustrated in Fig.10-(b). In addition, we find in both figures that the voltage passes across the initial value, and then restitutes to the initial value.

VI. CONCLUDING REMARKS

This paper has presented a novel tactile sensor-embedded soft fingertip (TES) where a micro force/moment sensing chip is used. This sensing chip is fabricated by using MEMS technology, and its strength is designed by FE analysis. We have shown the high sensitivity and performance of the sensor, and demonstrated that the response

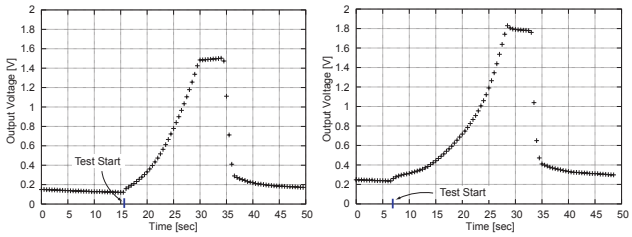

(a) Fz in $\theta_p = 0$ deg (b) Fz in $\theta_p = 20$ deg

Fig. 11. The results of Fz when the force is wholly applied to the fingertip up to 60 N.

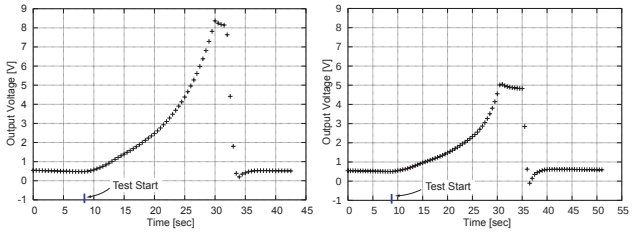

(a) Mx in $\theta_p = 20$ deg (b) My in $\theta_p = 20$ deg

Fig. 12. The results of Mx and My.

characteristics is superior in the dynamic sense. Finally, we have clarified that TES system is absolutely useful for robotic fingertips that is able to play as the perception like human fingers.

In future works, we are going to use the TES system to soft-fingered robotic hand, and achieve the dextrous manipulation with human-like tactile perception.

ACKNOWLEDGMENT

This research was supported in part by the Ritsumeikan University 21st Century COE program "Micro Nanoscience Integrated Systems".

REFERENCES

[1] T.Inoue and S.Hirai, "Local Minimum of Elastic Potential Energy on Hemispherical Soft Fingertip", *Proc. IEEE Int. Conf. on Robotics and Automation*, pp.2319-2324, 2005.

[2] T.Inoue and S.Hirai, "Study on Hemispherical Soft-Fingered Handling for Fine Manipulation by Minimum D.O.F. Robotic Hand", *Proc. IEEE Int. Conf. on Robotics and Automation*, which will be presented in Orlando, USA, 2006.

[3] Dzung Viet Dao, "Study on Silicon Piezoresistive Six-Degree of Freedom Micro Force-Moment Sensors and Application to Fluid Mechanics", *Doctoral thesis in Ritsumeikan University*, 2003.

[4] R.J.Roark, "Formulas for stress and strain", 4th Ed., *McGraw-Hill*, 1965.